Apoptosis (2019) 24:879–891
https://doi.org/10.1007/s10495-019-01566-4

Rotenone protects against β-cell apoptosis and attenuates type 1 diabetes mellitus

Mengqiu Wu[1,2,3,4] · Weiyi Chen[1,2,3] · Shengnan Zhang[1,2,3] · Songming Huang[1,2,3] · Aihua Zhang[1,2,3] · Yue Zhang[1,2,3] · Zhanjun Jia[1,2,3]

Published online: 4 September 2019

Abstract

Type 1 diabetes mellitus (T1DM) is caused by pancreatic β-cell dysfunction and apoptosis, with consequent severe insulin deficiency. Thus, β-cell protection may be a primary target in the treatment of T1DM. Evidence has demonstrated that defective mitochondrial function plays an important role in pancreatic β-cell dysfunction and apoptosis; however, the fundamental effect of mitochondrial complex I action on β-cells and T1DM remains unclear. In the current study, the pancreas protective effect of complex I inhibitor rotenone (ROT) and its potential mechanism were assessed in a streptozotocin (STZ)-induced mouse model of T1DM and in cultured mouse pancreatic β-cell line, Min6. ROT treatment exerted a hypoglycemic effect, restored the insulin level, and decreased inflammation and cell apoptosis in the pancreas. In vitro experiments also showed that ROT decreased STZ- and inflammatory cytokines-induced β-cell apoptosis. These protective effects were accompanied by attenuation of reactive oxygen species, increased mitochondrial membrane potential, and upregulation of transcriptional coactivator PPARα coactivator 1α (PGC-1α)-controlled mitochondrial biogenesis. These findings suggest that mitochondrial complex I inhibition may represent a promising strategy for β-cell protection in T1DM.

Keywords β-Cells · Mitochondrial complex I · Rotenone · Apoptosis · Type 1 diabetes mellitus

Introduction

Type 1 diabetes mellitus (T1DM) is a metabolic disorder characterized by polyuria, polydipsia, weight loss, and marked hyperglycemia. Distinguished from Type 2 diabetes mellitus, T1DM is typically considered to be inherited or induced by exposure to environmental triggers that alter the immune system and initiate destruction and apoptosis of β-cells, resulting in consequent severe insulin deficiency [1, 2].

Recent evidence suggests that mitochondrial dysfunction plays an important role in pancreatic β-cell dysfunction and apoptosis [3, 4]. The mechanisms may involve increased reactive oxygen species (ROS) production, impaired mitophagy, and liberation of pro-apoptotic proteins from the mitochondria [5–7]. In particular, abnormally elevated mitochondrial respiratory chain activity and increased oxidative stress have been demonstrated in the pancreas of T1DM animal models [8–10]. The mitochondrial respiratory chain is the major source of ROS [9]; therefore, inhibiting mitochondrial respiratory chain activity might be an effective approach to eliminate ROS, rebuild mitochondrial homeostasis, and protect β-cells from apoptosis. The respiratory chain consists of five linked membrane protein complexes named complex I, II, III, IV and V, of which ROS is mainly produced by complex I and III. Reports showed that complex III-derived ROS are predominantly released into the intermembrane space and may act as second messengers to target

✉ Yue Zhang
zyflora2006@hotmail.com

✉ Zhanjun Jia
jiazj72@hotmail.com; jiazhanjun72@njmu.edu.cn

1 Department of Nephrology, Children's Hospital of Nanjing Medical University, Guangzhou Road #72, Gulou District, Nanjing 210008, China

2 Jiangsu Key Laboratory of Pediatrics, Nanjing Medical University, Hanzhong Road #140, Gulou District, Nanjing 210029, China

3 Nanjing Key Laboratory of Pediatrics, Children's Hospital of Nanjing Medical University, Gulou District, Guangzhou Road #72, Nanjing 210008, China

4 State Key Laboratory of Kidney Diseases, Fuxing Road #28, Haidian District, Beijing 100853, China

proteins located in the mitochondrial matrix, intermembrane space, outer membrane, or cytosol; while complex I-derived ROS are completely released into the matrix, are less specific, and may contribute predominantly to oxidative stress [11–13]. Therefore, we hypothesized that complex I may be an optimum target for limiting toxic ROS production.

Rotenone (ROT), a proven mitochondrial complex I inhibitor, is a naturally occurring compound extracted from the roots and stems of *Lonchocarpus* and *Derris* species, and has been used extensively as an insecticide and to induce animal models of Parkinson's disease [14]. Although it has been considered toxic, ROT was recently discovered to be a protective agent in several disease models [15–21]. Hou et al. demonstrated that ROT could alleviate hyperglycemia in diabetic (db/db) mice via inducing glycolysis and reducing hepatic glucose output [15]. ROT was also shown to ameliorate lipopolysaccharide/D-galactosamine-induced fulminant liver injury in mice [16]. Moreover, a series studies from our group have shown the potential of ROT to attenuate vascular injury-induced neointimal hyperplasia [17], to protect against aldosterone, acetaminophen, ischemia/reperfusion, and chronic ureteral obstruction-induced renal injury [18–21], and to suppress deoxycorticosterone acetate-salt-induced hypertension in mice [22]. Another group reported the effects of inhibiting mitochondrial function on T helper cell differentiation, posing a potential influence on immune responses [23]. However, the role of ROT in T1DM has not been determined. Therefore, the present study aimed to determine the pancreas-protective effect of ROT in streptozotocin (STZ)-induced T1DM mice and to further verify the results in vitro using STZ- and inflammatory cytokines (cks) induced pancreatic Min6 β-cells.

Materials and methods

Chemicals and reagents

STZ, sodium citrate, citrate acid, ROT, mercapto-ethanol, dimethylsulfoxide (DMSO) and bovine serum albumin (BSA) were all purchased from Sigma-Aldrich (St Louis, MO, USA). Recombinant murine inflammatory cytokines interleukin I beta (IL-1β), tumor necrosis factor alpha (TNF-α) and interferon gamma (IFN-γ) were obtained from Peprotech (Rocky hill, NJ, USA). Glucose solution (200 g/L) was purchased from Gibco (Grand Island, NY, USA).

Animals

Healthy male C57BL/6 mice (7 weeks old, 20–24 g) were purchased from the Model Animal Research Center of Nanjing University (Nanjing, China) and were housed under standard laboratory conditions, with constant temperature (22 ± 2 °C), an automatic 12 h:12 h light/dark cycle, and allowed free access to water and food. All animal studies were approved by the Nanjing Medical University Institutional Animal Care and Use Committee.

Induction of type 1 diabetes in mice and rotenone treatment

A multiple low dose of STZ treatment protocol was used to induce T1DM in mice. Briefly, after 5 h of starvation, the mice received an intraperitoneal (i.p.) injection of sodium citrate buffer (pH 4.5), or STZ (50 mg/kg) dissolved in sodium citrate buffer (pH 4.5) for 5 consecutive days. One week after the final injection of STZ, mice with fasting blood glucose concentration ≥ 15 mM were included in the study. The diabetic mice were further randomly divided into an STZ group (n = 9) and an STZ + ROT group (n = 9) according to their blood glucose concentration (Fig. 1a).

ROT diet at a dose of 100 parts per million (ppm) was given to the mice in the STZ + ROT group 9 days after the final injection of STZ. The mice of Ctrl and STZ groups were treated with a diet without ROT during the same period. The body weight and blood glucose level of each mouse was recorded weekly. After 5 weeks of ROT treatment, all mice were sacrificed. Blood, pancreas and heart tissues were harvested for further analysis (Fig. 1a).

Enzyme-linked immunosorbent assay (ELISA) analysis of serum insulin levels

Serum samples were collected by centrifugation of whole blood at 1000×*g* for 10 min. Serum insulin levels were then quantified using a commercial mouse insulin ELISA kit (Elabscience Biotechnology, Wuhan, China) according to the manufacturer's instructions.

Histological and immunohistochemical analyses of islets

Pancreas tissues were fixed in 4% paraformaldehyde, dehydrated, embedded in paraffin, and cut into 4-μm slices for histological and immunohistochemical staining. Hematoxylin-eosin (H&E) staining was carried out using a commercial H&E staining kit (Solarbio life sciences, Beijing, China). Before immunohistochemistry, the slices were mounted on slides and then deparaffinized, rehydrated, and subjected to heat-induced antigen retrieval in improved citrate antigen retrieval solution (Beyotime Biotechnology, Shanghai, China) in a microwave oven. The slides were then incubated in 3% H_2O_2, blocked with 5% normal goat serum, and incubated with primary antibody against Insulin (Proteintech Group, Chicago, IL, USA) overnight in humidified chambers at 4 °C. After washing with phosphate-buffered saline (PBS)

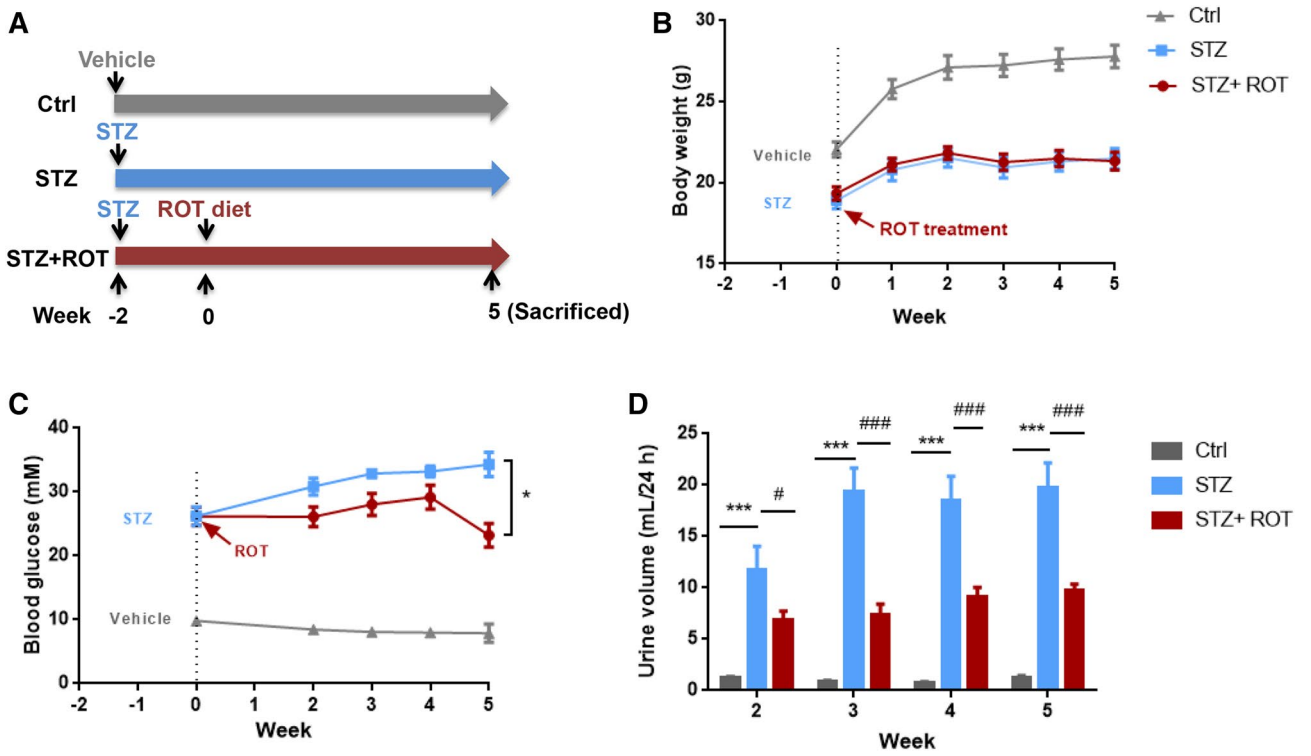

Fig. 1 Hypoglycemic effect of ROT in STZ-induced T1DM mice. **a** Schema illustrating the grouping of mice and rotenone intervention. After 5 consecutive days of STZ injection, mice with fasting blood glucose concentration ≥ 15 mM were included as type 1 diabetic mice. The diabetic mice were then randomized to receive a vehicle or rotenone (ROT, 100 ppm) containing gelled diet. All mice were sacrificed 5 weeks after treatment with ROT. **b**, **c** Body weight (**b**) and blood glucose levels (**c**) of the mice in each group. **d** 24-h Urine was collected weekly and the urine volume was recorded. Data are represented as mean ± SEM; * denotes $p < 0.05$ and *** denotes $p < 0.001$ when comparing to Ctrl group; # denotes $p < 0.05$ and ### denotes $p < 0.001$ when comparing to STZ group; $n = 7$ for Ctrl group and $n = 9$ for STZ and STZ + ROT groups.

three times, the sections were incubated with horseradish peroxidase at room temperature for 60 min. A commercial diaminobenzidine (DAB) kit (ZSbio, Beijing, China) was used to determine the localization of peroxidase conjugates. Sections were then stained with hematoxylin, dehydrated, and covered. Brown positive staining areas were captured under an Olympus BX51 microscope (Olympus, Center Valley, PA). Data were analyzed using the Image-Pro Plus 6.0 system (Media Cybernetic, Silver Springs, MD, USA).

Cell culture and treatment

The mouse pancreatic β-cell-derived cell line, Min6, was obtained from the American Type Culture Collection (Manassas, VA, USA) and cultured in Dulbecco's modified Eagle's medium (DMEM) (Gibco) supplemented with 100 U/mL penicillin, 100 μg/mL streptomycin, 15% (v/v) fetal bovine serum (Gibco) and 50 μM mercapto-ethanol at 37 °C with 5% CO_2. To determine the anti-apoptotic effects of ROT, cells were pre-treated with 1, 2, 5 or 10 nM ROT for 2 h, and then exposed to STZ (5 mM) or inflammatory cytokines (5 ng/mL IL-1β, 25 ng/mL TNF-α, and 25 ng/mL IFN-γ) for 24 h. Cells treated with 0.1% DMSO were used as controls.

Cell viability assay

Min6 cells were seeded at a density of 2×10^3/well in 96-well plates in serum-containing medium and treated with ROT at final concentrations of 1, 2.5, 5, 10, 20, 50, 75, 100, and 200 nM (0.1% DMSO). Cells treated with 0.1% DMSO were used as controls. Cell viability was assessed 24 h later using a Cell Counting Kit 8 (CCK8) (ApexBio, Houston, TX, USA) according to manufacturer's protocol. After incubation for 45 min at 37 °C, the absorbance was detected at 450 nm using a microplate reader Multiscan FC (Thermo Scientific, Waltham, MA, USA). Each assay was performed in four replicate wells and the relative cell viability was estimated by the relative ratio of each group to the control group.

Table 1 Sequences of the primers used for real-time PCR

Name	Forward primer (5'−3')	Reverse primer (5'−3')
Actb	GGCTGTATTCCCCTCCATCG	CCAGTTGGTAACAATGCCATGT
Il1b	ACTGTGAAATGCCACCTTTTG	TGTTGATGTGCTGCTGTGAG
Vcam	CGCTTCCGCTACCATCAC	GGCGGCTCAGTATCTCCTC
Bax	GATCAGCTCGGGCACTTTAG	TTGCTGATGGCAACTTCAAC
Bcl2	CTCAGGCTGGAAGGAGAAGAT	AAGCTGTCACAGAGGGGCTAC
Pgc1α	CAGGAACAGCAGCAGAGACA	GGAGTTGTGGGAGGAGTTAGG
ND1	ACACTTATTACAACCCAAGAA CACAT	TCATATTATGGCTATGGGTCAGG
ND2	CCATCAACTCAATCTCACTTC TATG	GAATCCTGTTAGTGGTGGAAGG
ND4	GCTTACGCCAAACAGAT	TAGGCAGAATAGGAGTGAT
ND5	GCCAACAACATATTTCAACTT TTC	ACCATCATCCAATTAGTAGAAAGGA
Cytb	GAGGTTGGTTCGGTTTTGG	GTTTTGAAAGGGTGGGTGAC
COX I	CAGACCGCAACCTAAACACA	TTCTGGGTGCCCAAAGAAT
COX II	GCCGACTAAATCAAGCAACA	CAATGGGCATAAAGCTATGG
COX III	CGTGAAGGAACCTACCAAGG	ATTCCTGTTGGAGGTCAGCA
ATPase6	CCATAAATCTAAGTATAGCCA TTCCAC	AGCTTTTTAGTTTGTGTCGGAAG
ATPase8	ACATTCCCACTGGCACC	GGGGTAATGAATGAGGC

Western blotting analysis

Pancreas tissues or Min6 cells were lysed using radioimmunoprecipitation assay (RIPA) lysis buffer in the presence of 1% protease inhibitors cocktail (Roche, Laval, Canada). The total protein level was then quantified using a commercial bicinchoninic acid (BCA) assay kit (Beyotime Biotechnology). Protein samples (50 μg) were separated using 8% or 10% SDS–PAGE, transferred onto polyvinylidene fluoride (PVDF) membranes, blocked overnight, incubated with primary antibodies, and subsequently with peroxidase tagged secondary antibodies (Beyotime Biotechnology). The resulting immunoreactive bands were detected using a chemiluminescence kit (Tiangen biotech, Beijing, China) on a ChemiDoc XRS$^+$ System (Bio-Rad, Hercules, CA, USA). The primary antibodies used included those recognizing: caspase 3 (Cell Signaling Technology, Danvers, MA, USA), cleaved caspase 3 (Cell Signaling Technology); Insulin (Proteintech Group) and peroxisome proliferator-activated receptor gamma coactivator 1-alpha (PGC-1α) (Santa Cruz Biotechnology, Santa Cruz, CA, USA). β-Actin (Proteintech) or glyceraldehyde-3-phosphate dehydrogenase (GAPDH) (Proteintech) were used as loading controls. The band intensities were quantified with the Image Lab software Version 3.0 (BioRad). Bands were framed manually with a rectangle tool and the average intensity of each band was recorded and normalized to loading controls.

Flow cytometry analysis of cell apoptosis

After treatment, cells were collected and labeled with Annexin V-fluorescein isothiocyanate (FITC)/propidium iodide (PI) (BD Biosciences, San Diego, CA, USA). After incubation for 15 min, cell fluorescent intensity was detected on a BD FACSCalibur instrument (Becton Dickinson, Franklin, NJ, USA). The annexin V positive subpopulation was recognized as apoptotic cells.

RNA isolation and quantitative real-time reverse transcription PCR (qRT-PCR)

Pancreas tissues were harvested and stored in Trizol reagent (Takara, Dalian, China). Total RNA was extracted using phenol chloroform extraction, precipitated in ethanol, and then subjected to reverse transcription using a PrimeScript RT Master Mix kit (Takara). qRT-PCR was subsequently carried out using SYBR Green PCR mix (Vazyme, Nanjing, China) on a 7500 Real Time PCR System (Applied Biosystems, Santa Clara, CA, USA). The primers used for amplification are listed in Table 1. Transcription levels were normalized to that of *Actb* (encoding β-Actin) and analyzed using the $2^{-\Delta\Delta Ct}$ method as is described previously [24].

Cellular reactive oxygen species assay

After treatment, cells were incubated with 10 μM 2′,7'-dichlorofluorescin diacetate (DCFH-DA) (Beyotime

Biotechnology) for 20 min at 37 °C. After incubation, the cells were washed three times with PBS and collected using trypsin digestion. DCFH-DA can be incorporated with the membrane-bound vesicles and converted to fluorescent product 2',7'-dichlorodihydrofluorescein (DCF). The fluorescence intensity of each sample was then analyzed using BD FACSCalibur (Becton Dickinson).

Mitochondria membrane potential analysis

The mitochondrial membrane potential assay kit with JC-1 (Beyotime Biotechnology) was used to analyze the mitochondrial membrane potential. After corresponding treatments, the cells were incubated with 5 mg/L JC-1 dye for 20 min at 37 °C and washed twice with the dye buffer. In cells with high mitochondrial membrane potential, JC-1-aggregates and forms red fluorescence (detected with excitation/emission wavelengths of 525/590 nm); while in cells with low mitochondrial membrane potential, JC-1 appears mainly in the monomer form with green fluorescence (detected with excitation/emission wavelengths of 490/530 nm). The mitochondrial membrane potential was expressed as the ratio of red fluorescence intensity over green fluorescence intensity.

Glucose-stimulated insulin secretion (GSIS) assay

Min6 cells were seeded onto 12-well plates until 60% confluent. After washing and 1 h preincubation in Kreb Ringer Hepes buffer (KRHB, pH 7.4; PanEra Biologicals, Guangzhou, China) supplemented with 2 mM glucose and 1 mg/mL BSA, cells were pretreated with ROT (5 or 10 nM) or vehicle (0.1% DMSO) for 1 h. Insulin secretion was stimulated by adding glucose to a concentration of 20 mM (high glucose, HG). Then the cells were incubated for 2 h and the supernatant was collected and centrifuged at 1000×*g* for 20 min at 4 °C to remove cell debris. The insulin secretion in medium was analyzed with a mouse insulin ELISA kit (Elabscience Biotechnology), and the cell lysis was used to measure inner cellular insulin level by Western blotting.

Assay of complex I activity of heart tissues

Due to the limited amount of pancreas tissue, the ROT effect on mitochondrial complex I activity in this experimental setting was detected in heart tissues using an assay kit purchased from Solarbio life sciences following the manufacturer's instructions. Heart tissues were homogenized on ice and centrifuged at 600×*g* for 10 min at 4 °C. The supernatant was then centrifuged at 11000×*g* for 10 min to isolate crude mitochondria. Mitochondria were extracted by resuspension of the mitochondrial pellet in mitochondrial lysis buffer and sonicating at 200 W, 3 s for 30 times on ice (Sonics, Connecticut, USA). Complex I activity was measured by mixing the resulting lysis with the reaction buffer provided in the kit. The initial absorbance values at 340 nm were recorded as A1 after the addition of reagents using a SpectraMAX 190 fluorometric plate reader (Molecular Devices, Sunnyvale, CA, USA). After incubation at 37 °C for 2 min, the absorbance values at 340 nm were recorded as A2. The activity of the mitochondrial complex-1 was calculated as the change of absorbance per minute per mg tissue protein and presented as U/mg protein.

Statistical analysis

Means ± SEM were used to present the data with the use of GraphPad Prism 7.0 software (La Jolla, CA, USA). Student's t-test was used for comparisons between two independent groups and one-way analysis of variance (ANOVA) followed by Bonferroni post hoc test was applied for comparisons among three or more groups. *P*-values less than 0.05 were considered significant.

Results

Hypoglycemic effect of rotenone in STZ-induced T1DM mice

To test the potential hypoglycemic effect of complex I inhibition in STZ-induced type 1 diabetic mice, a ROT diet at a dose of 100 ppm was given 9 days after the final STZ injection, when the fasting blood glucose level of all the included mice was above 15 mM (Fig. 1a). Weekly monitoring displayed no influence of ROT on the body weight of the mice compared with that in the STZ group (Fig. 1b). Strikingly, ROT significantly lowered the blood glucose level in the STZ-induced diabetic mice and the urine volume over 24 h decreased by more than a 50% during the 5-week experiment (Fig. 1c, d).

Rotenone treatment restored insulin levels in T1DM mice

Since the limited tissue availability of pancreas, complex I activity inhibition effect by rotenone was confirmed using isolated mitochondria from heart tissues. Elevated trend of complex-1 activity was seen in heart tissues of T1DM mice, which was entirely reversed by ROT treatment (Fig. 2a). Food intake within 24 h was measured, and the results showed comparable statistics between the STZ group and the STZ + ROT group (Fig. 2b). Thereafter, serum and pancreas islet insulin levels were detected separately (Fig. 2c–g). ROT upregulated the serum insulin level in the STZ-induced type 1 diabetic mice (Fig. 2c). Moreover, the immunostaining (Fig. 2d–e) and western blotting (Fig. 2f–g) results showed

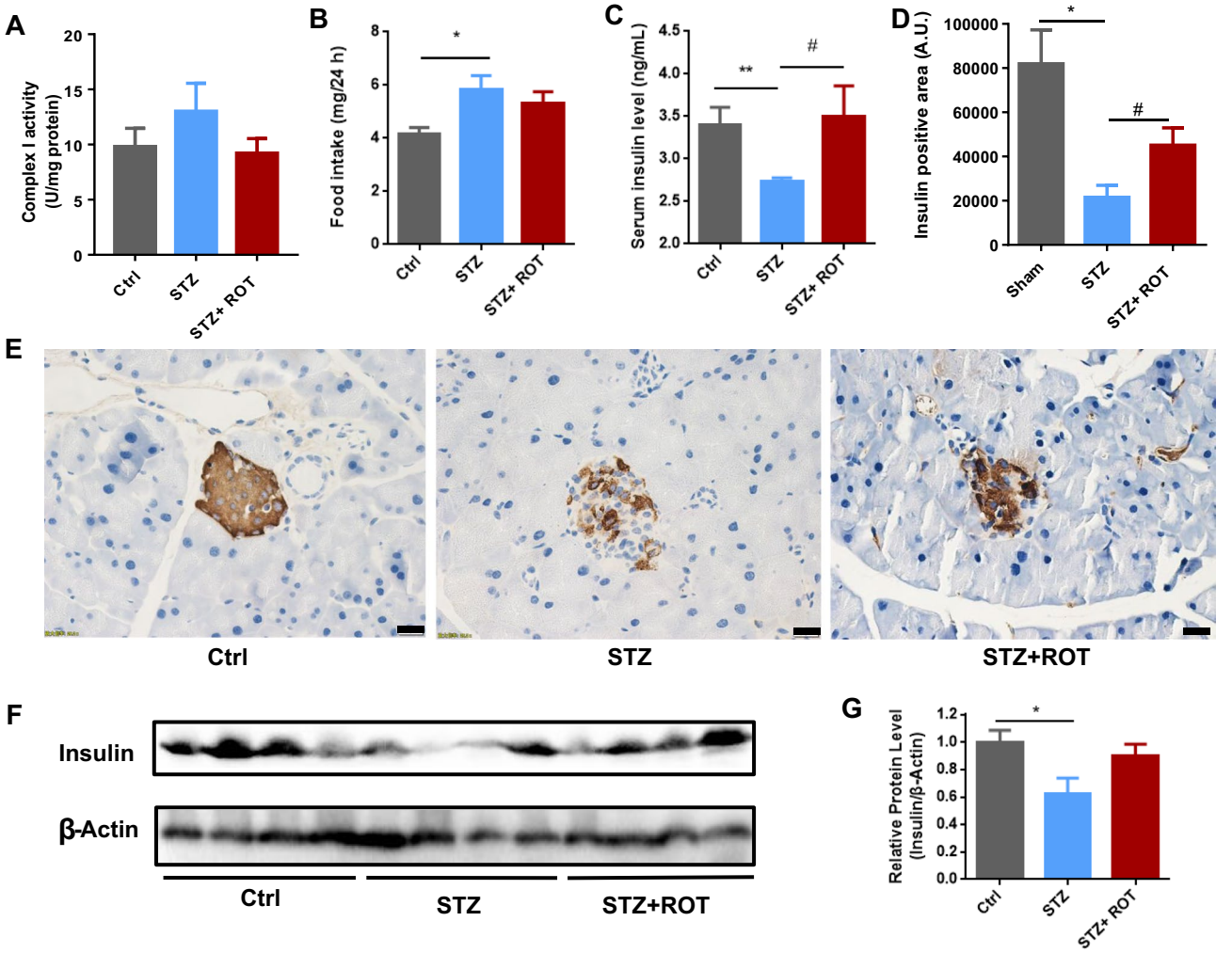

Fig. 2 Rotenone treatment restored insulin levels in T1DM mice. **a** Average complex I activity in isolated mitochondria from heart tissues of the indicated groups (n = 7 for Ctrl group and n = 9 for STZ and STZ + ROT groups). **b** Average food intake of mice from the indicated groups (n = 7 for Ctrl group and n = 9 for STZ and STZ + ROT groups). **c** ELISA analysis of serum insulin levels (n = 7 for Ctrl group and n = 9 for STZ and STZ + ROT groups). **d**–**e** Using IHC, insulin expression was assessed in the pancreas of control mice, STZ mice, and STZ + ROT mice. Magnification × 200; scale bars, 50 μm. Insulin positive areas were quantified in (D) (n = 6 ~ 7 for each group). **f**–**g** Using western blotting analysis, decreased insulin expression was observed in the pancreas of STZ mice, which was reversed by administration of ROT. The bar graphs in (**g**) represent the expression levels of the insulin relative to that of β-actin. Data are represented as mean ± SEM; * denotes $p < 0.05$ and ** denotes $p < 0.01$ when comparing to Ctrl group; # denotes $p < 0.05$ when comparing to STZ group.

higher insulin levels in pancreas of STZ + ROT group compared with that in the STZ group. These data indicated that ROT reduced the blood glucose level in STZ induced type 1 diabetic mice by re-establishing the pancreatic and circulating insulin levels.

Rotenone attenuated inflammation and the apoptotic response in pancreas of STZ-induced T1DM mice

The destruction of the insulin producing pancreatic β-cells is responsible for the onset of T1DM; therefore, we tested the effect of ROT on the inflammation and apoptosis level of pancreas tissue. By H&E staining of pancreas sections, immune cells were seen in the islets in STZ-treated mice, which was attenuated by ROT (Fig. 3a). Accordingly, qRT-PCR results showed that ROT could reverse the upregulated transcriptional levels of inflammatory cytokine IL-1β *(Il1b)* and vascular cell adhesion molecule *(Vcam)* (Fig. 3b, c). Meanwhile, ROT was also able to reverse the upregulation of proapoptotic gene *Bax* (BCL2 associated X, apoptosis regulator) and the downregulation of anti-apoptotic gene *Bcl2* (BCL2, apoptosis regulator) (Fig. 3d, e). Western blotting showed significantly

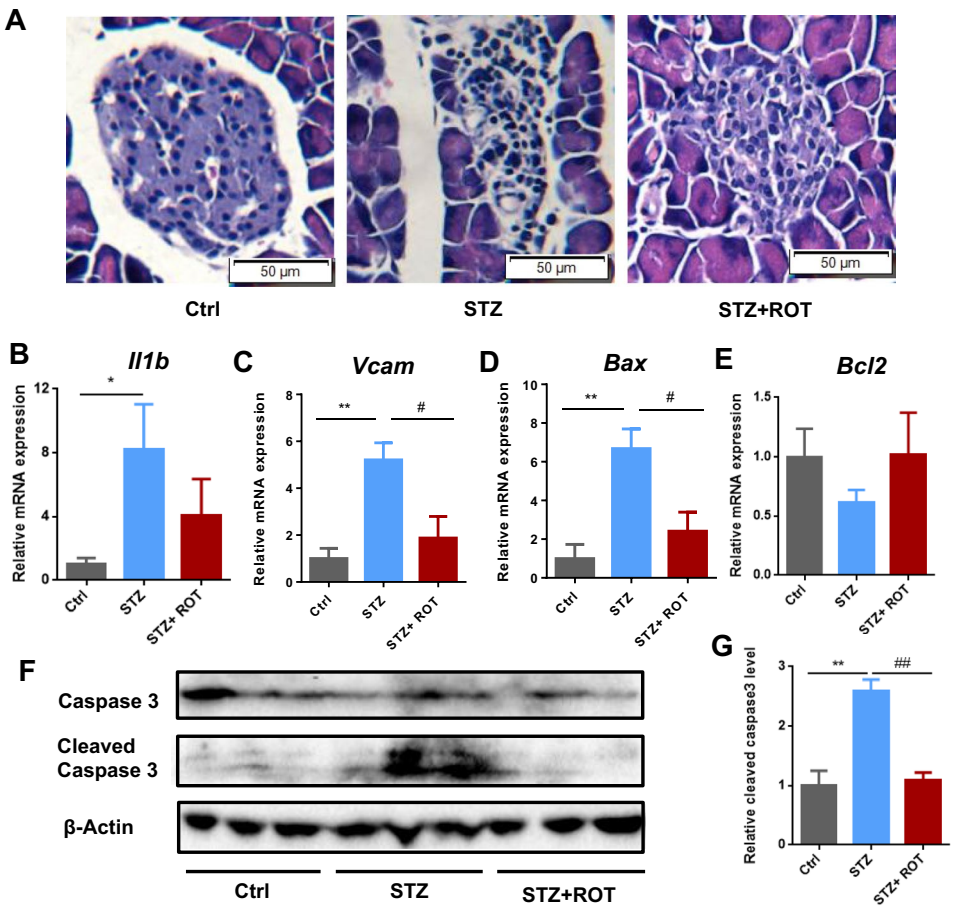

Fig. 3 Rotenone attenuated inflammation and apoptotic response in pancreas of STZ-induced T1DM mice. **a** Hematoxylin-eosin (H&E) staining of pancreatic sections (n = 7 for Ctrl group and n = 9 for STZ and STZ + ROT groups). Magnification × 200; scale bars, 50 μm. (B-E) qRT-PCR analysis of inflammatory cytokines *Il1b* (**b**) and *Vcam* (**c**), pro-apoptosis gene *BAX* (**d**) and anti-apoptosis gene *BCL-2* (**e**) (n = 6–9 in each group). **f–g** Western blots of pancreas proteins showing altered levels of cleaved caspase 3. The bar graphs in (**g**) represent the quantification of average band intensity of cleaved caspase 3 in (**f**). β-Actin was used as a loading control. Data are represented as mean ± SEM; * denotes $p < 0.05$ and ** denotes $p < 0.01$ when comparing to Ctrl group; # denotes $p < 0.05$ and ## denotes $p < 0.01$ when comparing to STZ group.

downregulated levels of cleaved caspase 3 in the pancreas of the STZ + ROT group compared with that in the STZ group (Fig. 3f, g). These results indicated that ROT had anti-inflammatory and anti-apoptotic actions in pancreas of type 1 diabetic mice.

Rotenone displayed no influence on glucose-stimulated insulin secretion (GSIS) in β-cells in vitro

As high concentration of ROT may impose toxic effects; therefore, it was necessary to ascertain the safe concentration of this agent in Min6 cells. Therefore, a CCK8 cell viability assay was performed to address this issue. Exposure of Min6 cells to various concentrations of ROT for 24 h showed that concentrations less than 75 nM had no significant influence on cell viability (Fig. 4a). Therefore, concentrations below 10 nM were used in the following in vitro experiments. To examine the influence of ROT on GSIS in Min6 β-cells, cultured Min6 β-cells were pretreated with ROT or 0.1% DMSO for 1 h and then exposed to low glucose (LG, 2 mM) or high glucose (HG, 20 mM) for 2 h. The supernatant medium was then collected for analysis of insulin secretion and the cell lysis was used to analyze inner cellular insulin level by Western blotting. Results showed that ROT posed no influence on insulin secretion (Fig. 4b) and inner cell insulin levels (Fig. 4c) at basal and high glucose conditions.

Rotenone ameliorated STZ- or inflammatory cytokines-induced β-cell apoptosis in vitro

We further verified the anti-apoptotic effect of ROT in vitro. Min6 β-cells challenged with STZ and inflammatory cytokines were used to mimic type 1 diabetic conditions. Annexin V-PI staining showed that ROT at 5 nM and 10 nM could efficiently protected against STZ-induced Min6 cell apoptosis, as indicated by the proportion of Annexin V positive cells in the ROT treated groups compared with that in the STZ group (Fig. 5a, b). Moreover, ROT could reduce the expression level of cleaved caspase 3 (Fig. 5c). Similar anti-apoptosis effects of ROT were detected in inflammatory cytokines-treated Min6 cells (Fig. 6a–c).

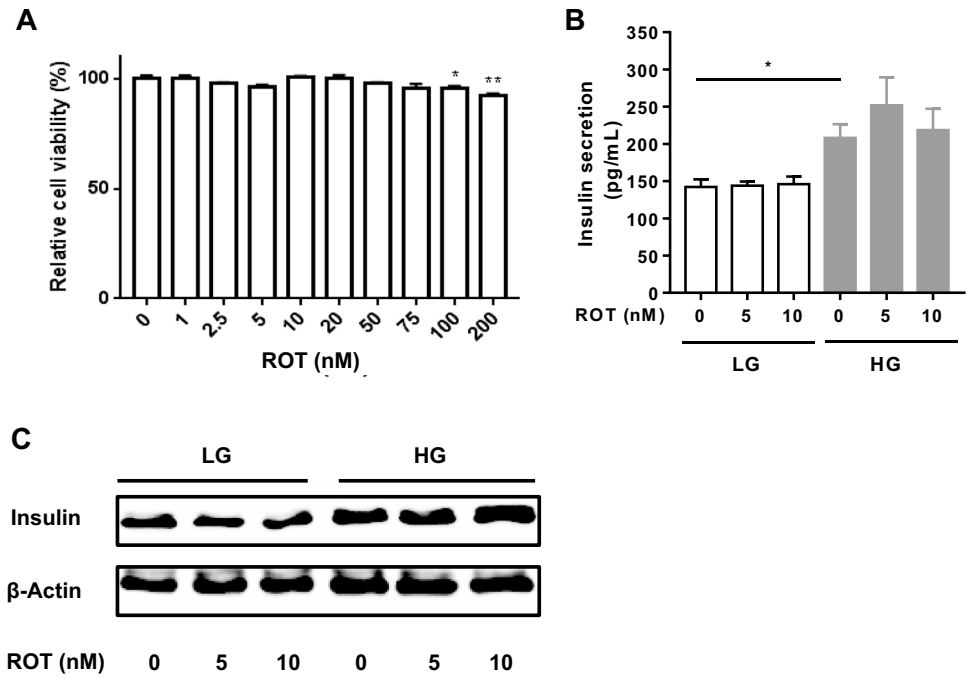

Fig. 4 Rotenone posed no influence on GSIS in Min6 β-cells. **a** Min6 cell viability after incubation with 0, 1, 2.5, 5, 10, 20, 50, 75, 100, and 200 nM ROT for 24 h was evaluated using a CCK8 kit (n = 4 for each group). **b** Effect of ROT (5 and 10 nM) on high glucose (HG, 20 mM)-induced insulin secretion. In low glucose (LG) groups, the concentration of glucose was 2 mM. Control cells were cultured in drug-free medium (0.1% DMSO) and collected for analysis at the same time (n = 3 for each group). **c** Relative inner cellular insulin levels were measured by Western blotting. β-Actin was used as a loading control. Data are represented as mean ± SEM; * denotes $p < 0.05$ comparing to Ctrl group

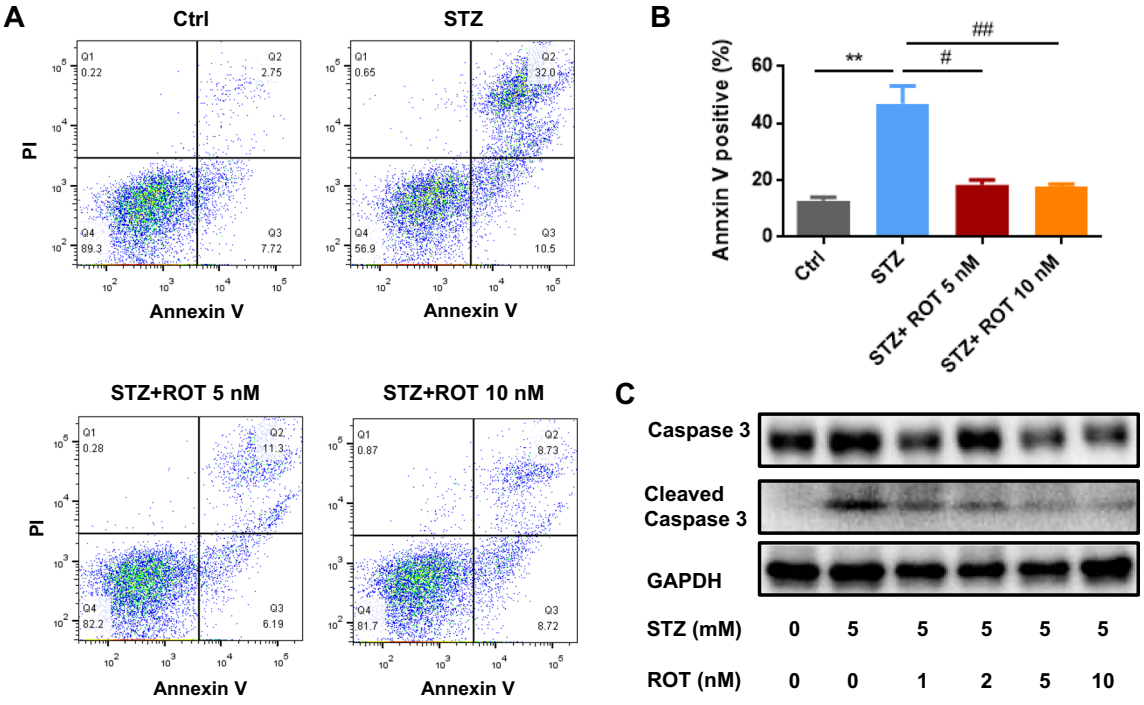

Fig. 5 Rotenone ameliorated STZ-induced β cell apoptosis in vitro. **a** Effect of ROT on STZ (5 mM)-induced cell apoptosis. Cellular apoptosis was measured using Annexin V-FITC/PI double staining at 24 h. Control cells were cultured in drug-free medium (0.1% DMSO) and collected for analysis at the same time. Annexin V positive cells were recognized as apoptotic cells and the rate is quantified in (**b**) (n = 3 for each group). **c** Western blotting analysis of caspase 3 and cleaved caspase 3 in Min6 cells under the indicated treatment. GAPDH was used as a loading control. Data are represented as mean ± SEM; ** denotes $p < 0.01$ when comparing to Ctrl group; # denotes $p < 0.05$ and ## denotes $p < 0.01$ when comparing to STZ group.

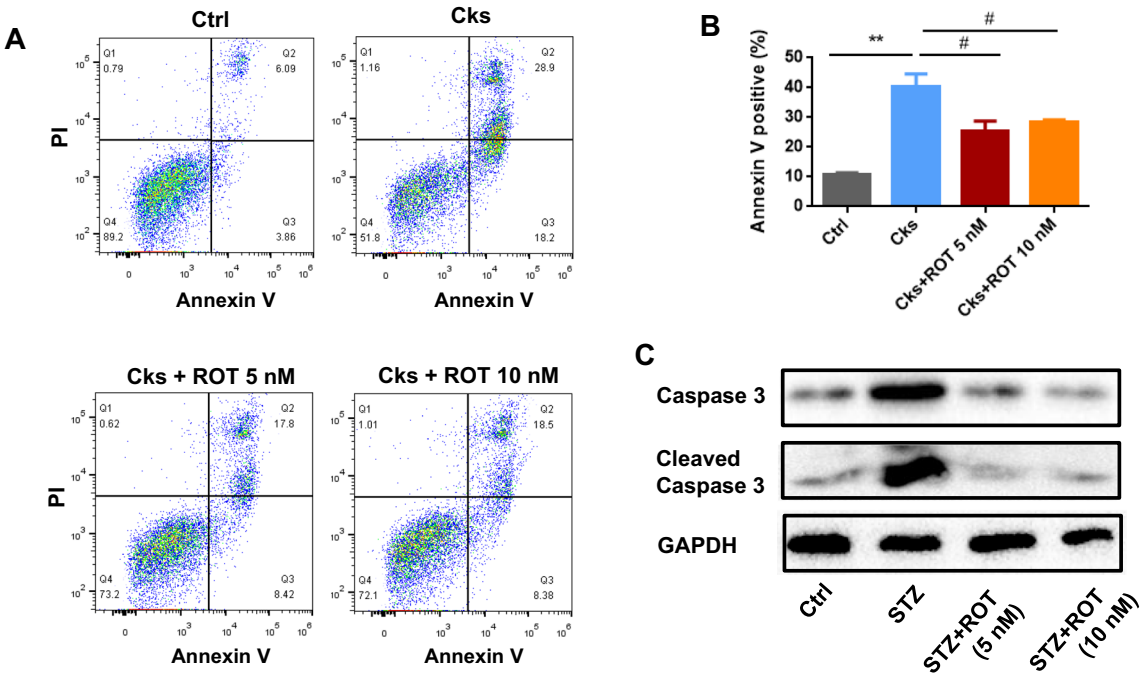

Fig. 6 Rotenone ameliorated inflammatory cytokines-induced β cell apoptosis in vitro. **a** Effect of ROT on inflammatory cytokines (cks) (5 ng/mL IL-1β,25 ng/mL TNF-α, and 25 ng/mL IFN-γ)-induced cell apoptosis. Cellular apoptosis was measured using Annexin V-FITC/PI double staining at 24 h. Control cells were cultured in drug-free medium (0.1% DMSO) and collected for analysis at the same time. The apoptotic rate is quantified in (**b**) (n = 3 for each group). **c** Western blotting analyses of caspase 3 and cleaved caspase 3 in Min6 cells under the indicated treatment. GAPDH was used as a loading control. Data are represented as mean ± SEM; ** denotes $p < 0.01$ when comparing to Ctrl group; # denotes $p < 0.05$ when comparing to Cks group.

Rotenone re-established mitochondrial homeostasis in β-cells

ROS are reported to be involved of in the development and progression of diabetes; therefore, assays were performed to measure the oxidative stress within cells. A significant increase of intracellular ROS levels was observed after STZ or inflammatory cytokines treatment, which was remarkably decreased by ROT treatment (Fig. 7a, b). Together with the attenuation of toxic ROS, ROT treatment significantly increased the mitochondrial membrane potential compared with that in inflammatory cytokines-treated cells (Fig. 7c). The transcriptional coactivator PGC-1α is the mitochondrial biogenesis regulator; therefore, we checked the expression level of PGC-1α. A reduction in the mRNA and protein levels of PGC-1α was observed after STZ treatment, which was significantly recovered by ROT treatment (Fig. 7d, e). We also detected the expression of 10 mitochondria encoded PGC-1α target genes involved in respiration chain (genes encoding complex I subunits: ND1, ND2, ND4 and ND5; complex III subunit: Cytb; complex IV subunits: COX I, COX II and COX III; complex V subunits: ATPase 6 and ATPase 8) in pancreatic tissue, which showed expression trends in line with that of PGC-1α (Fig. 7f).

Discussion

T1DM progression is characterized by the dysfunction and apoptosis of pancreatic β-cells [1, 2]. Defective mitochondrial function, especially elevated complex I activity and increased oxidative stress, has been demonstrated in the pancreas of T1DM animal models [8–10]. Hence, we inferred that inhibiting the overactive complex I might help to rebuild mitochondrial homeostasis, protect β-cells from apoptosis, and thus alleviate T1DM.

ROT is a known complex I inhibitor that has been used extensively to induce animal models of Parkinson's disease (PD). However, the administration route reported for ROT-based PD models is mainly parenteral; oral route delivery usually does not induce obvious neurotoxic effects [25]. Accordingly, we and other groups did not find any hepatic or renal toxicity of ROT at 200 or 600 ppm delivered via oral chow in mice [17, 21, 19, 20, 22]. In addition, in a recently published paper, ROT at 400 ppm was administered to mice through diet for up to 14 days followed by a safety profile assessment. Histopathological evaluations and gene expression analysis revealed no obvious neurotoxic effect [26]. The weak neurotoxic effect of oral ROT might be explained by its poor bioavailability. ROT is incompletely absorbed in

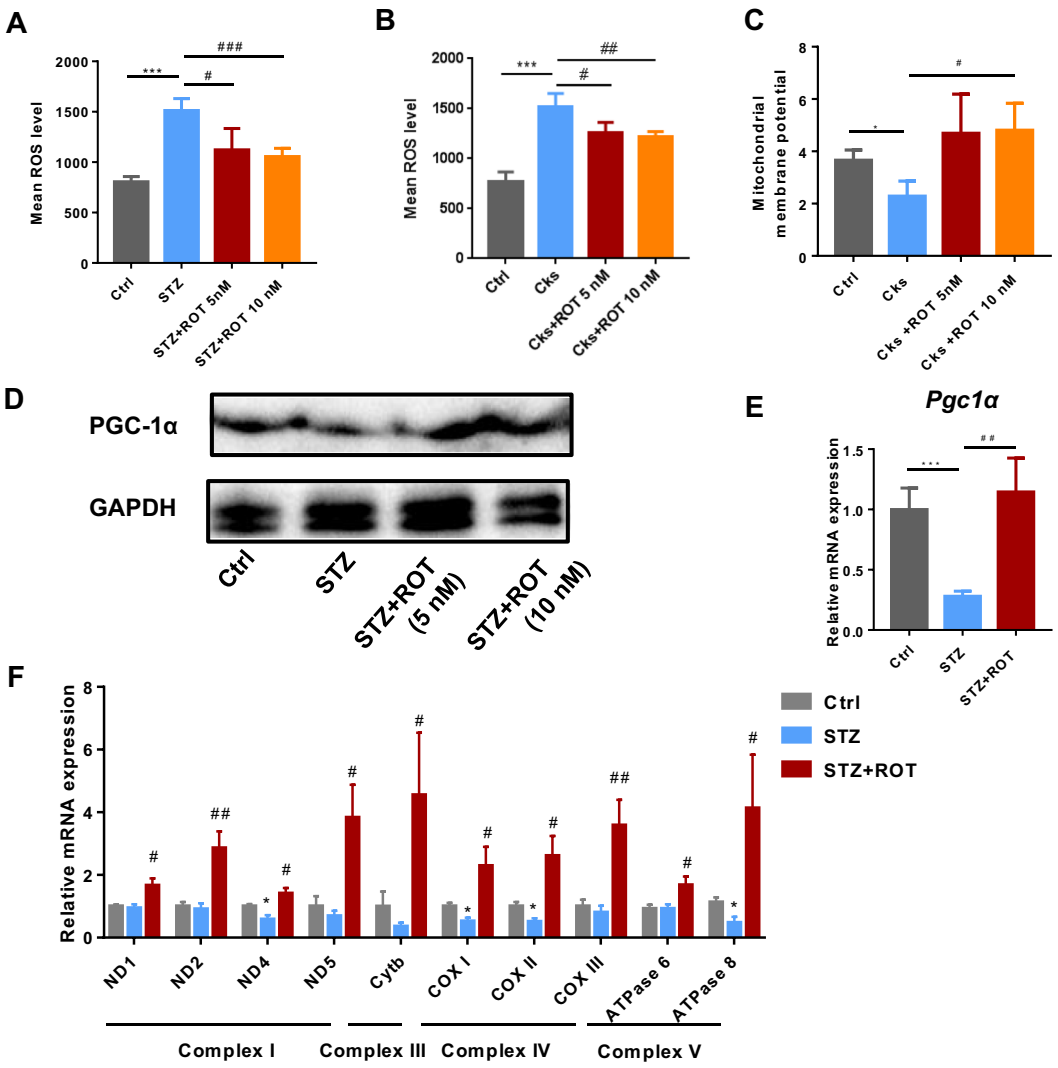

Fig. 7 Rotenone attenuated ROS levels, increased mitochondrial membrane potential, and stimulated the expression of PGC-1α and mitochondrial biogenesis. **a**, **b** Effect of ROT on the cellular ROS level. Cells were stimulated with STZ (5 mM) (**a**) or cytokines (cks) (5 ng/mL IL-1β, 25 ng/mL TNF-α, and 25 ng/mL IFN-γ) (**b**) for 24 h with or without ROT. Control cells were cultured in drug-free medium (0.1% DMSO) and collected for analysis at the same time. Cellular ROS was estimated by incubation with DCFH-DA (10 μM) followed by flow cytometry analysis and the mean ROS level is quantified (n = 4 for each group). **c** Effect of ROT on the mitochondrial membrane potential. Mitochondrial membrane potential was detected by incubating with JC-1 (5 mg/L), followed by detection on a fluorescence microplate reader (n = 3 for each group). **d** Western blotting analysis of PGC-1α in Min6 cells under the indicated treatment. GAPDH was used as a loading control. **e**, **f** qRT-PCR analysis of PGC-1α and PGC-1α target genes (complex I subunits: ND1, ND2, ND4 and ND5; complex III subunit: Cytb; complex IV subunits: COX I, COX II and COX III; complex V subunits: ATPase 6 and ATPase 8) in the pancreas of control mice, STZ mice, and STZ + ROT mice (n = 6–9 in each group). Data are represented as mean ± SEM; * denotes $p < 0.05$ and *** denotes $p < 0.001$ when comparing to Ctrl group; # denotes $p < 0.05$, ## denotes $p < 0.01$ and ### denotes $p < 0.001$ when comparing to STZ or Cks groups.

the stomach and intestine and is metabolized in the liver [27, 26]. As a result, after oral ROT intake of low dosage, brain ROT exposure levels were not sufficient to alter mitochondrial respiration and cause neurotoxicity [28]. Besides neurotoxicity, high concentration of ROT may also cause oxidative stress and cell death in peripheral tissues [29]. Based on the published toxic and therapeutic evaluation of ROT [17, 21, 19, 20, 22, 26], we propose that treatment with relatively low dose of ROT (< 250 ppm, around < 40 mg/kg/day) through oral route might impose periphery therapeutic effect and avoid neurotoxic effects. However, more efforts are still needed to modify the chemical structure of ROT or other complex I inhibitors to limit their neurotoxic. In the present study, ROT at a dosage of 100 ppm was administrated through oral route in T1DM mice.

To assess the effect of ROT on T1DM mice, multiple low-dose STZ was injected via i.p. to establish a mouse T1DM model. STZ, an analog of N-acetylglucosamine, can selectively enter β-cells via glucose transporter 2 to cause cell destruction via DNA alkylation, representing an important tool in developing T1DM animal models [30]. STZ-induced diabetic mice showed hyperglycemia, polyuria, reduced body weight, and typical apoptotic and inflammatory changes in the pancreas. ROT treatment for 5 weeks started after completing STZ injection for 9 days, significantly improved the polyuria and hyperglycemia symptoms in T1DM, with no influence on body weight. ROT could also reverse the decreased insulin level in the serum and pancreas. The decreased blood glucose and increased insulin level probably resulted from ROT's protection of the pancreas, as shown by improved inflammation and apoptosis in the pancreas of the STZ + ROT group compared with that of the STZ group. To further assess the effect of ROT on insulin secreting β-cells, the Min6 cell line was induced by STZ and inflammatory cytokines to mimic the T1DM conditions. Annexin V-PI staining and the expression of pro-apoptosis markers (cleaved caspase 3) in both conditions revealed that ROT at concentrations below 10 nM showed protective effect against β-cell apoptosis.

Furthermore, inhibiting complex I activity using ROT could significantly attenuate the intracellular ROS level and increase the mitochondrial membrane potential of Min6 cells treated with STZ or inflammatory cytokines. In line with our results, recent research also proved that reducing mitochondrial complex I activity via NADH dehydrogenase [ubiquinone] 1 alpha subcomplex subunit 4-like 2 (NDUFA4L2) could limit intracellular ROS production [31]. Another group claimed that metformin and ROT could ameliorate arsenic trioxide hepatotoxicity by inhibiting mitochondrial complex I and decreasing intracellular ROS levels [32]. In addition to ROS, it has been proven that mitochondrial biogenesis is critical for maintaining mitochondrial function in β-cells in health and disease [33]. Mitochondrial biogenesis is mainly activated by the transcriptional coactivator PGC-1α, which functions by promoting mitochondrial DNA (mtDNA) transcription and replication [34, 35]. Notably, reduced expression of PGC-1α and its responsive oxidative phosphorylation (OXPHOS) genes has been observed in patients with type 2 diabetes, implicating impaired mitochondrial biogenesis in diabetes [36]. In the current study, we found that the expression level of PGC-1α was downregulated by STZ and was rescued by ROT treatment in Min6 cells. Upregulated PGC-1α further stimulated mitochondrial biogenesis, as evidenced by the upregulated mRNA levels of PGC-1α-targeted mitochondrial genes. Taken together, these results indicated that the complex I inhibitor ROT protects β-cell from apoptosis by restricting the production of ROS and by stimulating mitochondrial biogenesis via upregulation of PGC-1α.

Previous studies showed that mitochondrial complex I inhibition alleviated hyperglycemia in T2DM mice by inducing glycolysis in the liver and muscles, ameliorating gluconeogenesis in hepatocytes [15], preventing lipid accumulation, and attenuating TNF-α-induced insulin resistance in vitro [37]. In a related paper we published recently, we found that post treatment of ROT after final STZ injection for 4 weeks had no effect on blood glucose levels while protected against diabetic kidney injury [38], indicating that an early ROT intervention on β-cell injury in diabetes is of importance. Moreover, the beneficial effects of PGC-1α stimulation in protecting kidney tubular cell in diabetic kidney disease [39], alleviating cardiac dysfunction in diabetic cardiomyopathy mice [40], and orchestrating functional angiogenesis in skeletal muscle of diabetic mice [41] have been demonstrated. These evidences strongly suggested that complex I inhibition together with PGC-1α stimulation might represent a promising strategy to treat diabetes and vascular complications.

Acknowledgements This work was supported by grants from the National Natural Science Foundation (Nos. 81800599, 81830020, 81873599, 81600352, 81670678, 81530023), the Natural Science Foundation of Jiangsu Province (No. BK20180145), the China Postdoctoral Science Foundation (No. 2018M632342) and Nanjing City Key Medical Research Project (No. ZKX18039).

Author Contributions Z.J., Y. Z., S.H., and A.Z coordinated and oversaw the study. M.W., W.C., and S.Z. performed the experiments, collected the samples, and analyzed the data. M.W., Y. Z., and Z.J. wrote the manuscript.

Compliance with ethical standards

Conflict of interest The authors declare no competing financial interest.

Ethical approval All animal experiments are in accordance with International Guidelines and Protocols and approved by the Nanjing Medical University Institutional Animal Care and Use Committee.

References

1. Chiang JL, Kirkman MS, Laffel LM, Peters AL, Sourcebook A (2014) Type 1 diabetes. Type 1 diabetes through the life span: a position statement of the American Diabetes Association. Diabetes Care 37(7):2034–2054. https://doi.org/10.2337/dc14-1140
2. Bluestone JA, Herold K, Eisenbarth G (2010) Genetics, pathogenesis and clinical interventions in type 1 diabetes. Nature 464(7293):1293–1300. https://doi.org/10.1038/nature08933
3. Supale S, Li N, Brun T, Maechler P (2012) Mitochondrial dysfunction in pancreatic beta cells. Trends Endocrinol Metab 23(9):477–487. https://doi.org/10.1016/j.tem.2012.06.002
4. Lee JW, Kim WH, Lim JH, Song EH, Song J, Choi KY, Jung MH (2009) Mitochondrial dysfunction: glucokinase downregulation

lowers interaction of glucokinase with mitochondria, resulting in apoptosis of pancreatic beta-cells. Cell Signal 21(1):69–78. https://doi.org/10.1016/j.cellsig.2008.09.015
5. Jung HS, Chung KW, Won Kim J, Kim J, Komatsu M, Tanaka K, Nguyen YH, Kang TM, Yoon KH, Kim JW, Jeong YT, Han MS, Lee MK, Kim KW, Shin J, Lee MS (2008) Loss of autophagy diminishes pancreatic beta cell mass and function with resultant hyperglycemia. Cell Metab 8(4):318–324. https://doi.org/10.1016/j.cmet.2008.08.013
6. Nishikawa T, Araki E (2007) Impact of mitochondrial ROS production in the pathogenesis of diabetes mellitus and its complications. Antioxid Redox Signal 9(3):343–353. https://doi.org/10.1089/ars.2007.9.ft-19
7. Gurzov EN, Eizirik DL (2011) Bcl-2 proteins in diabetes: mitochondrial pathways of beta-cell death and dysfunction. Trends Cell Biol 21(7):424–431. https://doi.org/10.1016/j.tcb.2011.03.001
8. Raza H, Prabu SK, John A, Avadhani NG (2011) Impaired mitochondrial respiratory functions and oxidative stress in streptozotocin-induced diabetic rats. Int J Mol Sci 12(5):3133–3147. https://doi.org/10.3390/ijms12053133
9. Brand MD, Affourtit C, Esteves TC, Green K, Lambert AJ, Miwa S, Pakay JL, Parker N (2004) Mitochondrial superoxide: production, biological effects, and activation of uncoupling proteins. Free Radic Biol Med 37(6):755–767. https://doi.org/10.1016/j.freeradbiomed.2004.05.034
10. Gerber PA, Rutter GA (2017) The role of oxidative stress and hypoxia in pancreatic beta-cell dysfunction in diabetes mellitus. Antioxid Redox Signal 26(10):501–518. https://doi.org/10.1089/ars.2016.6755
11. St-Pierre J, Buckingham JA, Roebuck SJ, Brand MD (2002) Topology of superoxide production from different sites in the mitochondrial electron transport chain. J Biol Chem 277(47):44784–44790. https://doi.org/10.1074/jbc.M207217200
12. Xu X, Arriaga EA (2009) Qualitative determination of superoxide release at both sides of the mitochondrial inner membrane by capillary electrophoretic analysis of the oxidation products of triphenylphosphonium hydroethidine. Free Radic Biol Med 46(7):905–913. https://doi.org/10.1016/j.freeradbiomed.2008.12.019
13. Bleier L, Wittig I, Heide H, Steger M, Brandt U, Drose S (2015) Generator-specific targets of mitochondrial reactive oxygen species. Free Radic Biol Med 78:1–10. https://doi.org/10.1016/j.freeradbiomed.2014.10.511
14. Xiong N, Long X, Xiong J, Jia M, Chen C, Huang J, Ghoorah D, Kong X, Lin Z, Wang T (2012) Mitochondrial complex I inhibitor rotenone-induced toxicity and its potential mechanisms in Parkinson's disease models. Crit Rev Toxicol 42(7):613–632. https://doi.org/10.3109/10408444.2012.680431
15. Hou WL, Yin J, Alimujiang M, Yu XY, Ai LG, Bao YQ, Liu F, Jia WP (2018) Inhibition of mitochondrial complex I improves glucose metabolism independently of AMPK activation. J Cell Mol Med 22(2):1316–1328. https://doi.org/10.1111/jcmm.13432
16. Ai Q, Jing Y, Jiang R, Lin L, Dai J, Che Q, Zhou D, Jia M, Wan J, Zhang L (2014) Rotenone, a mitochondrial respiratory complex I inhibitor, ameliorates lipopolysaccharide/D-galactosamine-induced fulminant hepatitis in mice. Int Immunopharmacol 21(1):200–207. https://doi.org/10.1016/j.intimp.2014.04.028
17. Yin J, Xia W, Wu M, Zhang Y, Huang S, Zhang A, Jia Z (2019) Inhibition of mitochondrial complex I activity attenuates neointimal hyperplasia by inhibiting smooth muscle cell proliferation and migration. Chem Biol Interact 304:73–82. https://doi.org/10.1016/j.cbi.2019.03.002
18. Hua H, Ge X, Wu M, Zhu C, Chen L, Yang G, Zhang Y, Huang S, Zhang A, Jia Z (2018) Rotenone protects against acetaminophen-induced kidney injury by attenuating oxidative stress and inflammation. Kidney Blood Press Res 43(4):1297–1309. https://doi.org/10.1159/000492589
19. Ding W, Xu C, Wang B, Zhang M (2015) Rotenone attenuates renal injury in aldosterone-infused rats by inhibiting oxidative stress, mitochondrial dysfunction, and inflammasome activation. Med Sci Monit 21:3136–3143. https://doi.org/10.1038/nature08933
20. Sun Y, Zhang Y, Zhao D, Ding G, Huang S, Zhang A, Jia Z (2014) Rotenone remarkably attenuates oxidative stress, inflammation, and fibrosis in chronic obstructive uropathy. Mediators Inflamm 2014:670106. https://doi.org/10.1155/2014/670106
21. Zhang W, Sha Y, Wei K, Wu C, Ding D, Yang Y, Zhu C, Zhang Y, Ding G, Zhang A, Jia Z, Huang S (2018) Rotenone ameliorates chronic renal injury caused by acute ischemia/reperfusion. Oncotarget 9(36):24199–24208. https://doi.org/10.18632/oncotarget.24733
22. Zhang A, Jia Z, Wang N, Tidwell TJ, Yang T (2011) Relative contributions of mitochondria and NADPH oxidase to deoxycorticosterone acetate-salt hypertension in mice. Kidney Int 80(1):51–60. https://doi.org/10.1038/ki.2011.29
23. Ozay EI, Sherman HL, Mello V, Trombley G, Lerman A, Tew GN, Yadava N, Minter LM (2018) Rotenone treatment reveals a role for electron transport complex I in the subcellular localization of key transcriptional regulators during T helper cell differentiation. Front Immunol 9:1284. https://doi.org/10.3389/fimmu.2018.01284
24. Livak KJ, Schmittgen TD (2001) Analysis of relative gene expression data using real-time quantitative PCR and the 2(-Delta Delta C(T)) Method. Methods 25(4):402–408. https://doi.org/10.1006/meth.2001.1262
25. Johnson ME, Bobrovskaya L (2015) An update on the rotenone models of Parkinson's disease: their ability to reproduce the features of clinical disease and model gene-environment interactions. Neurotoxicology 46:101–116. https://doi.org/10.1016/j.neuro.2014.12.002
26. Heinz S, Freyberger A, Lawrenz B, Schladt L, Schmuck G, Ellinger-Ziegelbauer H (2017) Mechanistic investigations of the mitochondrial complex I inhibitor rotenone in the context of pharmacological and safety evaluation. Sci Rep 7:45465. https://doi.org/10.1038/srep45465
27. Bove J, Prou D, Perier C, Przedborski S (2005) Toxin-induced models of Parkinson's disease. NeuroRx 2(3):484–494. https://doi.org/10.1602/neurorx.2.3.484
28. Sherer TB, Betarbet R, Testa CM, Seo BB, Richardson JR, Kim JH, Miller GW, Yagi T, Matsuno-Yagi A, Greenamyre JT (2003) Mechanism of toxicity in rotenone models of Parkinson's disease. J Neurosci 23(34):10756–10764. https://doi.org/10.1523/JNEUROSCI.23-34-10756.2003
29. Greenamyre JT, Betarbet R, Sherer TB (2003) The rotenone model of Parkinson's disease: genes, environment and mitochondria. Parkinsonism Relat Disord 9(Suppl 2):S59–S64. https://doi.org/10.1016/S1353-8020(03)00023-3
30. Furman BL (2015) Streptozotocin-induced diabetic models in mice and rats. Curr Protoc Pharmacol 70:5 47 41 – 20. https://doi.org/10.1002/0471141755.ph0547s70
31. Zhang H, Gong G, Wang P, Zhang Z, Kolwicz SC, Rabinovitch PS, Tian R, Wang W (2018) Heart specific knockout of Ndufs4 ameliorates ischemia reperfusion injury. J Mol Cell Cardiol 123:38–45. https://doi.org/10.1016/j.yjmcc.2018.08.022
32. Ling S, Shan Q, Liu P, Feng T, Zhang X, Xiang P, Chen K, Xie H, Song P, Zhou L, Liu J, Zheng S, Xu X (2017) Metformin ameliorates arsenic trioxide hepatotoxicity via inhibiting mitochondrial complex I. Cell Death Dis 8(11):e3159. https://doi.org/10.1038/cddis.2017.482
33. Mulder H (2017) Transcribing beta-cell mitochondria in health and disease. Mol Metab 6(9):1040–1051. https://doi.org/10.1016/j.molmet.2017.05.014

34. Li PA, Hou X, Hao S (2017) Mitochondrial biogenesis in neurodegeneration. J Neurosci Res 95(10):2025–2029. https://doi.org/10.1002/jnr.24042
35. Scarpulla RC (2002) Nuclear activators and coactivators in mammalian mitochondrial biogenesis. Biochim Biophys Acta 1576(1–2):1–14. https://doi.org/10.1016/s0167-4781(02)00343-3
36. Mootha VK, Lindgren CM, Eriksson KF, Subramanian A, Sihag S, Lehar J, Puigserver P, Carlsson E, Ridderstrale M, Laurila E, Houstis N, Daly MJ, Patterson N, Mesirov JP, Golub TR, Tamayo P, Spiegelman B, Lander ES, Hirschhorn JN, Altshuler D, Groop LC (2003) PGC-1alpha-responsive genes involved in oxidative phosphorylation are coordinately downregulated in human diabetes. Nat Genet 34(3):267–273. https://doi.org/10.1038/ng1180
37. Leonard S, Tobin LM, Findlay JB (2017) The signalling mechanisms of a novel mitochondrial complex I inhibitor prevent lipid accumulation and attenuate TNF-alpha-induced insulin resistance in vitro. Eur J Pharmacol 800:1–8. https://doi.org/10.1016/j.ejphar.2017.01.007
38. Wu M, Li S, Yu X, Chen W, Ma H, Shao C, Zhang Y, Zhang A, Huang S, Jia Z (2019) Mitochondrial activity contributes to impaired renal metabolic homeostasis and renal pathology in STZ-induced diabetic mice. Am J Physiol Renal Physiol. https://doi.org/10.1152/ajprenal.00076.2019
39. Yuan S, Liu X, Zhu X, Qu Z, Gong Z, Li J, Xiao L, Yang Y, Liu H, Sun L, Liu F (2018) The role of TLR4 on PGC-1alpha-mediated oxidative stress in tubular cell in diabetic kidney disease. Oxid Med Cell Longev 2018:6296802. https://doi.org/10.1155/2018/6296802
40. Ma S, Feng J, Zhang R, Chen J, Han D, Li X, Yang B, Li X, Fan M, Li C, Tian Z, Wang Y, Cao F (2017) SIRT1 activation by resveratrol alleviates cardiac dysfunction via mitochondrial regulation in diabetic cardiomyopathy mice. Oxid Med Cell Longev 2017:4602715. https://doi.org/10.1155/2017/4602715
41. Rowe GC, Raghuram S, Jang C, Nagy JA, Patten IS, Goyal A, Chan MC, Liu LX, Jiang A, Spokes KC, Beeler D, Dvorak H, Aird WC, Arany Z (2014) PGC-1alpha induces SPP1 to activate macrophages and orchestrate functional angiogenesis in skeletal muscle. Circ Res 115(5):504–517. https://doi.org/10.1161/CIRCRESAHA.115.303829